Pergamon

Geochimica et Cosmochimica Acta, Vol. 63, No. 15, pp. 2183–2198, 1999

0016-7037/99 $20.00 + .00

PII S0016-7037(99)00193-3

The chemistry of lava–seawater interactions: The generation of acidity

JOSEPH A. RESING*,[1] and FRANCIS J. SANSONE[2]

[1]Pacific Marine Environmental Laboratory, National Oceanic and Atmospheric Administration, Seattle, Washington 98115, USA
[2]Department of Oceanography, School of Ocean Earth Sciences and Technology, University of Hawaii, Honolulu, Hawaii 96822, USA

(*Received January* 2, 1998; *accepted in revised form May* 17, 1999)

Abstract—High concentrations of acid were found to arise from the interaction between molten rock and seawater at the shoreline of Kilauea Volcano, Hawaii. A series of field samplings and experiments show that the acid was derived from two sources: the release of magmatic volatiles and water–rock reactions. Although the bulk of the magmatic volatiles (CO_2, H_2O, and SO_2) are vented at Puu Oo cinder cone before the lava's transit downslope to the ocean, a portion of the sulfur (S) and fluoride (F) gasses are retained by the lava and then are released partially when the lava is quenched by seawater. The primary water–rock reaction responsible for acid formation appears to be Na-metasomatism, which is much different from the predominant acid-forming reaction found in submarine hydrothermal systems, Mg-metasomatism. Analyses of surface seawater and of precipitation (rain) deposited at the shore show that ~30% of the acid comes from magmatic gasses with the balance from reactions between the rock and the salts found in seawater. Experimental results show that ~4 ± 1.5 mEq of acid are formed per kilogram of lava entering the ocean, and of this 1 ± 0.5 mEq/kg of lava came from S and F, with the balance coming from water–rock reactions. On the basis of lava extrusion rates, ~200–720 × 10^6 Eq/yr of acid are being formed at this site. The deposition of the acid results in the alteration of subaerial lava flows along the coast, and the lowering of the pH of the adjacent surface ocean waters by more than 1 unit. The ejection of this acid into the atmosphere contributes to the formation of an extensive haze downwind of the lava entries.

1. INTRODUCTION

Submarine volcanism is the predominant form of volcanism on the surface of the earth (Crisp, 1984), occurring predominantly at mid-ocean ridge (MOR) spreading centers and hotspot submarine volcanos. Although there have been extensive investigations of hydrothermal fluids created during the interaction between hot rock and seawater (e.g., Von Damm, 1990 and references therein), there have been few studies of the physical and geochemical effects of direct lava–seawater interaction. The study presented here is the most extensive investigation to date of the aqueous geochemistry of the interaction between molten rock and seawater. It was conducted at the shoreline of Kilauea Volcano, Hawaii, where lava has been entering the ocean on a fairly continuous basis since 1986. The geochemical signature observed in this setting is distinct when compared with other forms of water–rock interaction and provides insight into the fundamental reactions that take place when molten rock and seawater interact. Submarine neovolcanism is an important process due to its frequency of occurrence in both the contemporary and ancient oceans. This report is aimed at understanding the geochemical consequences of interaction between molten rock and seawater.

During this study, it was observed that large amounts of acid were created when lava and seawater made contact. Observed decreases in pH in waters near submarine volcanos during both eruptive and noneruptive phases have been largely linked to the direct venting of magmatic gasses to the surrounding seawater (Gamo et al., 1987; Cheminée et al., 1991; Sedwick et al., 1992; Resing and Sansone, 1996). The largest influence on pH generally arises from the magmatic CO_2, and to a lesser degree from magmatic SO_2 with minor additions from HF and HCl. However, the volatiles originally present in Kilauea's magma are generally thought to be degassed subaerially at Puu Oo cinder cone before reaching the ocean (Gerlach and Taylor, 1990). It was postulated, therefore, that the origin of the acid at the shoreline of Kilauea Volcano was from water–rock reactions, with the reaction mechanism being the instantaneous evaporation of seawater and precipitation of solid $MgCl_2$ followed by "dry steam reaction" to form $HCl_{(g)}$ and $Mg(OOH)_{2(s)}$ or $MgO_{(s)}$ (Gerlach et al., 1989). Additional support for the Mg-metasomatism during lava–seawater interactions was provided by Sedwick et al. (1991) who suggested that Mg-metasomatism was responsible for the generation of acid in samples collected above submarine lava flows at the shoreline of Kilauea.

The results presented here suggest that there are two distinct mechanisms for the formation of acidity when there is direct contact between molten rock and seawater: (1) the emanation of residual acidic–magmatic volatiles from the lava and (2) the generation of acidity through Na-metasomatism. These results show that magmatic S and F gasses have not been removed completely from the lava before its transit down the slopes of Kilauea and into the ocean. In addition, the predominance of Na-metasomatism over that of Mg-metasomatism is likely due to the greater abundance of Na^+ over that of Mg^{2+} in seawater combined with the speed, pressure, and temperature of the reactions taking place.

We investigated the generation of acidity during lava–seawater interactions using both field and experimental data. The first part of the study involved collecting seawater samples and hydrographic data at the site where lava entered the ocean. The second was the collection and analysis of precipitation that was

*Author to whom correspondence should be addressed (E-Mail: resing@pmel.noaa.gov).

deposited beneath the large steam plumes created when lava entered the ocean. The third was a series of experiments in which a measurable quantity of molten lava was reacted with a known volume of water.

2. BACKGROUND

2.1. Chemistry

The generation of acidity from seawater–rock reactions is a fairly well-documented process in both natural and experimental hydrothermal systems (e.g., Seyfried and Mottl, 1995 and references therein). The initial reaction that occurs is the removal of Mg^{2+} to create $Mg(OH)_2$-silicate phases, with the release of H^+ to solution (e.g., Bischoff and Dickson, 1975), where the net reaction is:

$$Mg^{2+} + 2H_2O \rightarrow Mg(OH)_{2(s)} + 2H^+. \quad (1)$$

In reviewing hydrothermal chemistry, Seyfried and Mottl (1995) observe that in experimental work, as temperatures increase above 350°C and the Mg^{2+} has been consumed, there is an increased tendency for exchange reactions to take place in which Na^+ is removed from solution to form H^+ (see also Mottl and Holland, 1978; Seyfried and Janecky, 1985; Shanks and Seyfried, 1987; Berndt et al., 1989). A relative decrease in Na^+ (when compared to Cl^-) has also been observed in hydrothermal fluids from several different settings (Butterfield et al., 1990; Butterfield and Massoth, 1994; Trefry et al., 1994; Von Damm et al., 1997), and in each of these systems Mg^{2+} concentrations were assumed to be zero, and it was generally assumed that Mg^{2+} metasomatism took place before that of Na^+ and Ca^{2+}.

In addition to seawater–rock reactions, magmatic gasses are rich in acidic volatiles (HF, HCl, HBr, SO_2, H_2S, and S_2) (Gerlach, 1993), and are the primary source of acidity in fumarolic condensates at most volcanos (e.g., Symonds et al., 1994). These magmatic gasses, when dissolved in water, contribute to acidity. The S within the lava is present as $SO_{2(g)}$, $S_{2(g)}$, $H_2S_{(g)}$, (Gerlach, 1993), and as $MeSO_4$ compounds, where Me is a cation. These compounds generate acidity in solution as follows:

$$4SO_2 + 4H_2O \rightarrow H_2S + 3H_2SO_4 \quad (2)$$

$$H_2S + 2O_2 \rightarrow SO_4^{2-} + 2H^+ \quad (3)$$

$$3H_2SO_4 \rightarrow 3SO_4^{2-} + 6H^+ \quad (4)$$

$$S_2 + 2H_2O + 3O_2 \rightarrow 4H^+ + 2SO_4^{2-} \quad (5)$$

where each of the reduced sulfur gasses produces 1 SO_4^{2-} and 2 H^+ per S. The F is present in the lava primarily as $HF_{(g)}$ and MeF compounds (Symonds et al., 1994). These compounds dissociate in water as follows:

$$HF \rightarrow H^+ + F^- \quad (6)$$

$$MeF_n \rightarrow Me^{n+} + nF \quad (7)$$

Of Kilauea's magmatic gasses, (excluding CO_2 and H_2O), the sulfur gasses are the most abundant with total S emissions 40–100 times greater than those of the halogens (Greenland, 1984; Gerlach, 1993). The gaseous emissions of both HCl and HF appear to be approximately equal with ranges of HCl:HF from 0.3:1 to 3:1 (Greenland, 1984; Miller et al., 1990). HBr emissions appear to be negligible, with F:Br ranging from 200:1 to 1000:1 in magmatic gasses from Kilauea (Miller et al., 1990). Although the vast bulk of Kilauea's magmatic gasses are vented at Puu Oo before the transport of its lava downslope to the ocean, the lava does retain some of the volatile phases (Greenland et al., 1985; Cashman et al., 1994). Greenland et al. (1985) estimated that after the initial degassing $<3\%$ of CO_2, 22% of S, 90% of Cl, and 98% of F are retained by the magma. The retention of magmatic gasses is also supported by the work of Cashman et al. (1994) who determined that $\sim 10\%$ of the S is retained in the lavas found on the flow field near the ocean entries.

2.2. Volcanism

The interaction between lava and seawater has been a common phenomenon throughout the history of the earth. In the present day ocean $>80\%$ of the global magmatism is manifest at the MORs in the deep ocean. In the geologic past, however, the largest known eruptions of lava are those referred to as large igneous provinces (LIPs), which include continental flood basalts, large oceanic platforms, and the massive outpourings of lava that took place at the advent of the formation of ocean basins (Coffin and Eldholm, 1994 and references therein). In addition to these immense eruptions of lava, many of the seamounts in the Pacific Ocean are thought to have erupted from 120 to 50 Ma near the surface of the ocean and subsequently, have subsided deep beneath the sea surface.

Oceanic plateaus are the largest of the LIPs and there is considerable evidence that most of these plateaus were produced from submarine volcanic activity, with much of it taking place at or near the surface of the ocean. For example, the emplacement of the Manihki Plateau (66 Ma) was interpreted to have taken place by volcanic activity at or near sea surface (Schlanger et al., 1981; Beirsdorf et al., 1995) as suggested by the 1150 km^3 volcaniclastic layer extending over an area of 5000 km^2 on the eastern part of the plateau (Beirsdorf et al., 1995). Similarly the Kereguelen Plateau currently has two active subaerial volcanos and it is believed that much of the plateau was emplaced near the surface ocean (Coffin and Eldholm, 1994). The largest of the oceanic plateaus, the Ontong-Java Plateau is thought to have been emplaced in water depths estimated to be between 1000 and 3000 m. However, the presence of volcaniclastic sediments suggests that near-surface ocean volcanism was taking place at seamounts on the plateau at the time of its emplacement (Tarduno et al., 1991).

The opening of ocean basins are associated with massive outpourings of lava, both as continental flood basalts and as ocean basin based eruptions (White, 1989; White and McKenzie, 1989; Eldholm and Thomas, 1993; Holbrook and Kelemen, 1993). White and McKenzie (1989) showed that most of the known episodes of continental rifting resulted in volcanism and this volcanism took place near sea level and subsequently subsided beneath the sea surface. The opening of the South Atlantic created massive volcanism that is responsible for the formation of the Paraná and Etendeka flood basalt provinces in South America and Central Africa, respectively. As the continents spread, the associated volcanism was responsible for the

formation of the Rio Grande Rise and Walvis Ridge, two ridges that are thought to have formed at or around sea level and have subsequently subsided (White and McKenzie, 1989). In the North Atlantic, the formation of the Voring Plateau was accompanied by voluminous volcanic activity along the ~3000 km rifted plate boundary. The oldest emplaced oceanic crust was emplaced close to sea level and the eruption center subsided beneath the surface of the ocean with waning sporadic volcanism (Eldholm and Thomas, 1993). Similarly, the formation of the Indian ocean was initiated with the formation of the Deccan Flood Basalt Province. Seaward dipping reflectors on the eastern part of the province suggests a substantial submarine component to the emplacement of the Deccan Trap. As the basin spread, the eruption center left a trail of volcanic ridges extending from the eastern edge of the province to the Mascarene plateau (Coffin and Eldholm, 1994). Much of the volcanism that formed these ridges is believed to have taken place at or near sea level. This brief history illustrates that the formation of the ocean basins was associated with large volumes of volcanic activity that were believed to have been emplaced near sea level.

Volcanism is also thought to have occurred in the mid-Pacific on an enormous scale between 110 and 70 Ma (Schlanger et al., 1981). It is believed that a mantle plume beneath the thin oceanic crust forced uplift of the seafloor, with the majority of seamount volcanism taking place near sea level. Since this time these seamounts have been subsiding and riding the Pacific plate to the north west (Schlanger et al., 1981).

In the present day ocean, the amount of near surface–ocean volcanic activity is less than in the geological past; however, the emergence of Surtsey from beneath the Atlantic Ocean in the 1960s provided a glimpse into the dramatic processes that took place in the geological past. The eruption was a spectacular event producing vertical columns of pyroclasts intermixed with seawater and steam that extended up to 1000 m high. This eruption undoubtably produced a large volume of aerosol particles that were rich in seasalt, basaltic glass, and the reaction products of lava–seawater interactions. These aerosols were likely spread a great distance, slowly raining out over a wide area of the North Atlantic.

Currently, the majority of volcanism takes place at MOR spreading centers (Crisp, 1984) 1 to 4 km beneath the surface of the ocean. Most of this MOR volcanism takes place at the fastest spreading ridges in the Pacific at ~2 km water depth. Seafloor eruptions at these depths are characterized by extensive sheet flows and pillow basalts with only very small amounts of hyaloclastites formed by violent eruption (Cas, 1992).

3. GEOGRAPHIC SETTING

The Puu Oo eruption of Kilauea Volcano on the southeast coast of the island of Hawaii is responsible for the shoreline and near-shore lava flows that enter the ocean at this site. Magma injected from the mantle forms a magma chamber beneath Kilauea caldera; this magma moves down Kilauea's east rift zone, where it initially reaches the earth's surface at Puu Oo cone. The bulk of the magmatic gasses and other volatiles are thought to be vented to the atmosphere at Puu Oo and to a lesser extent at Kilauea Caldera (Gerlach and Taylor, 1990). Upon reaching the surface at Puu Oo, the lava is transported down slope both as surface flows and through subsurface lava tubes, with the latter being the primary mechanism for the transport of lava to low lying regions and to the ocean (Mattox et al., 1993; Peterson et al., 1994). Some lava tubes are thought to continue beneath the ocean surface to feed at least some of the underwater flows observed farther offshore (Peterson, 1976; Tribble, 1991). The eruption producing these flows began on January 3, 1983, and extruded lava at an average rate in excess of 3×10^5 m^3/d over the period 1983–1991 (Wolfe et al., 1987; Heliker and Wright, 1991; Mattox et al., 1993). During mid-1989, the average lava extrusion rate from Kilauea Volcano was 2.5 to 3.0×10^5 m^3/d, with ~20 to 30% of the lava entering the ocean at one or more locations (Kelly et al., 1989). Also, from April to October, 1991, during a period of declining flow, $\sim 1.8 \times 10^5$ m^3/d of lava was being erupted (Kauahikaua et al., 1996) and ~36% of the lava was estimated by Harris et al. (1998) to reach the ocean whereas Kauahikaua et al. (1996) estimated that closer to 100% entered the ocean.

The lava temperatures measured for the current eruption range from 1130°C (Helz et al., 1995) to 1150°C (Cashman et al., 1994). The vesicularity of lavas from surface outbreaks has been found to range from 50–88% (Cashman et al., 1994).

The entry of lava into the ocean is often a violent process as molten lava is rapidly quenched and fractured by the relatively cool seawater. In turn, the lava heats the seawater creating a large pool of warm water with very distinctive hydrographic features (see Sansone and Resing, 1995; Resing, 1997). Large steam plumes are created where the lava enters the ocean by the rapid heating and vaporization of seawater from the quenching and cooling of molten lava. These vigorous steam plumes are centered at the flow front and their bases are as wide as the flow front. As these plumes rise they expand laterally and disperse downwind. During normal trade wind conditions these plumes are pushed along and over the coastal area creating hazy conditions as they disperse. A portion of this steam immediately recondenses and falls as highly saline and acidic precipitation. As this precipitation dries, it creates a whitish halo on the subaerial flow field centered near the ocean entry. The white color arises from both the evaporation of the saline precipitation and alteration of the basalt by acidity in these fluids. The processes responsible for the formation of the precipitation include the condensation of vapor within the vapor-saturated plume, the coagulation of small droplets onto glassy particles and other salt-rich droplets, and spatter from the intense physical interaction of lava and seawater. The precipitation falls most heavily within 20 to 30 m of where the lava enters the ocean, often falling as intense but sporadic downpours.

4. METHODS

4.1. Sample Collection

All samples, except where noted, were filtered in the field using 0.2 μm pore size acid-washed polycarbonate Nuclepore filters in acid-washed Nuclepore in-line filtration rigs. Filtration was accomplished by subsampling the sample bottle or experimental container using acid-washed 50 mL high density polyethylene syringes. The syringes were rinsed three times with sample and then used to force the sample through the filter. The first 25 to 50 mL of filtrate was passed to waste to rinse the filter. Finally, each acid-washed sample bottle was rinsed three times with filtered sample. All acid-washed plasticware was washed as described by Resing (1997). Sample bottles for alkalinity

Table 1. Summary of experiments performed in this study.

Sample name	Composition	Mass of lava (kg)	Water volume (L)	Mass/volume (kg/L)	T_0 (°C)	T_f (°C)	ΔT (°C)
			March 10, 1995, SW Day 1				
301	SW	0.031	1.50	0.021	29	34	5
302	SW	0.275	1.50	0.183	21	67	46
304	SW	0.086	1.50	0.057	27	42	15
306	SW	0.250	1.50	0.167	26	63	37
308	SW	0.679	1.50	0.453	31	101*	70
310	SW	0.276	1.50	0.184	24	63	39
			March 11, 1995, SW Day 2				
309	SW	0.228	1.50	0.152	20	57	37
311	SW	0.283	1.50	0.189	21	60	39
318	SW	0.200	1.50	0.133	20	56	36
319	SW	0.242	1.50	0.162	20	56	36
			August 15, 1995, August DIW				
807	DIW	0.120	1.00	0.120	34	60	26
810	DIW	0.259	1.00	0.259	33	90	57
802	DIW	0.138	1.00	0.138	34	66	32
814	DIW	0.069	1.00	0.069	33	49	16
809	DIW	0.440	1.00	0.440	32	100*	69
			October 12, 1995, Acid experiments				
1001	NaCl	0.168	0.91	0.185	32	75	43
1002	$MgCl_2$–NaCl	0.269	0.87	0.309	33	101*	68
1003	$MgSO_4$–NaCl	0.166	0.85	0.196	33	80	47
1004	DIW	0.201	0.93	0.216	33	78	45
1005	Na_2SO_4–NaCl	0.129	0.91	0.142	33	69	36
1006	SW	0.127	0.90	0.141	37	73	36
			October 13, 1995, October DIW				
1007	DIW	0.131	1.50	0.088	33	53	20
1008	DIW	0.476	1.49	0.321	38	90	52
1009	DIW	0.214	1.50	0.143	34	64	30
1010	DIW	0.228	1.48	0.154	37	70	33
1025	SW	0.294	1.51	0.195	26	72	46

* The water in these experiments boiled.
T_0 = initial temperature; T_f = the final temperature; $\Delta T = T_f - T_0$; SW = seawater; DIW = Deionized water.

and pH were washed with soap and water and rinsed three times with >17 MΩ deionized water (DIW). Precipitation from the steam plume was collected on acid-washed polyethylene sheets, which were 0.5 mm thick. These sheets were soaked in 10% HCl for >48 h and then rinsed with DIW, and allowed to dry. All acid washing was carried out in class-100 clean conditions.

4.1.1. Surface ocean

Ocean-based sampling was undertaken from a 24-ft fishing boat. Samples discussed here were collected on four different dates: March 20, 1990, September 23 and 24, 1990, and March 1, 1991. Specific sampling locations and site details are described by Sansone and Resing (1995). Samples were taken using a polyethylene bottle placed at the end of a 1.5 m acrylic "pole sampler." Immediately upon collection samples were filtered and subsamples were taken for trace element analysis, nutrients, and alkalinity. Unfiltered samples were taken for pH and "total" elemental concentrations. Samples for dissolved gas analysis were collected with a peristaltic pump connected to a 7-mm internal diameter polypropylene tubing extending ~50 cm below the sea surface.

4.1.2. Precipitation

Samples of precipitation were collected on three occasions, February 28, 1991, January 31, 1995, and March 11, 1995, by placing acid-washed plastic sheets below the steam plume within 10 to 20 m of the lava entry. Precipitation was significant enough at times to collect >1 L in less than 10 min from a 1 m^2 area. Within minutes of their accumulation, the samples were collected and filtered (except as noted below). Filtration took 5 to 10 min. On February 28, 1991, two samples (91-6 and 91-7) were collected and a combination of safety factors precluded the filtering of these samples. An additional three samples (95-1, 95-2, and 95-3) were collected in January 1995 and another sample (95-16) was collected in March 1995. In January and March 1995 the sheets were rinsed once with precipitation by pouring freshly collected precipitation off the sheet to waste before samples were collected.

4.1.3. Experiments

To better understand the chemical interaction between molten lava and seawater, a series of experiments was conducted in which measurable quantities of lava were placed in known volumes of water of various compositions. We report the results of 26 different experiments from five different days that were conducted using seawater, DIW, and various salt solutions (Table 1). Individual experiments were conducted by taking lava from a subaerial lava flow and placing it into water contained in a 2 L polyethylene bowl with a tight-sealing lid (kitchenware). The lid of the container was manually held onto the container during the most vigorous interactions. When the visible interactions had ceased, the solution was stirred by swirling the water in the container until a stable temperature was reached. For the seawater experiments, open-ocean surface seawater from the north central Pacific Ocean (Hawaii Ocean Time Series station) was used. For the DIW and salt solution experiments, ≥17 MΩ DIW was used. Subsampling and filtration were conducted in a similar manner as that for the ocean samples. Water temperature was measured using a Teflon-coated K-type junction thermocouple and lava temperatures were measured using a chrome-alumel K-type junction thermocouple.

The different experiments are discussed below. In general we observed two broadly classified lava flow types: fluid and fast moving,

Table 2. Generation of acid from placing lava into different solutions.

	Starting Conditions					Results		
Experiment	$[Cl^-]$ (mmol/L)	$[Na^+]$ (mmol/L)	$[Mg^{2+}]$ (mmol/L)	$[SO_4^{2-}]$ (mmol/L)	Carbonate alkalinity (mEq/L)	Decrease in alkalinity (mEq/L)	Acidity per amount of lava (mEq/kg)†	ΔT (°C)
1001 NaCl	520	520	0	0	1.97	0.46	2.3	43
1002 $MgCl_2$–NaCl*	610	520	49	0	1.92	1.93	5.7	68
1003 $MgSO_4$–NaCl	520	520	49	50	1.98	0.49	2.3	47
1004 DIW	0	2	0	0	1.97	0.04	0.18	45
1005 Na_2SO_4–NaCl	520	620	0	50	1.94	0.66	4.3	36
1006 Seawater	530	471	53	28	2.27	0.36	2.2	36

* The water in this experiment boiled for several minutes.
† Decrease in alkalinity divided by lava concentration from Table 1.

and viscous and slow moving. Lava was collected from the flow front using either the crook end of a crow bar or a large stamped metal spoon.

4.1.3.1. March 10, 1995 (SW—day 1). Seven experiments were conducted on an active part of the flow field that formed a broad front >200 m across. In these experiments varying amounts of molten lava as single blobs were added to a constant volume of seawater (see Table 1). The solutions were filtered within 40 to 120 min of the completion of each experiment. The lava was very fluid and fast moving on this day.

4.1.3.2. March 11, 1995 (SW—day 2). Four experiments were conducted near those of March 10 to test the effects of varying lava surface area on the extent of reaction. In each of these experiments multiple blobs of molten lava were added to a constant volume of seawater using the crook end of a crow bar to collect the lava. Samples were filtered within 40 to 120 min of the completion of each experiment. The lava on this day was viscous and slow moving.

4.1.3.3. August 15, 1995 (August DIW). Six experiments were conducted at a flow field that was >200 m across with multiple flow fronts at ~150 m above sea level. The lava at this site was very fluid and fast moving. Multiple blobs of molten lava were collected using the crook end of a crow bar and placed into a fixed volume of DIW. Samples were filtered within 10 to 30 min of the completion of each experiment.

4.1.3.4. October 12, 1995 (acid experiments). Six experiments were conducted to examine the effects of different salt solutions on the formation of acidity. The compositions of the solutions are shown in Table 2. NaCl was added so that each of the solutions had the same

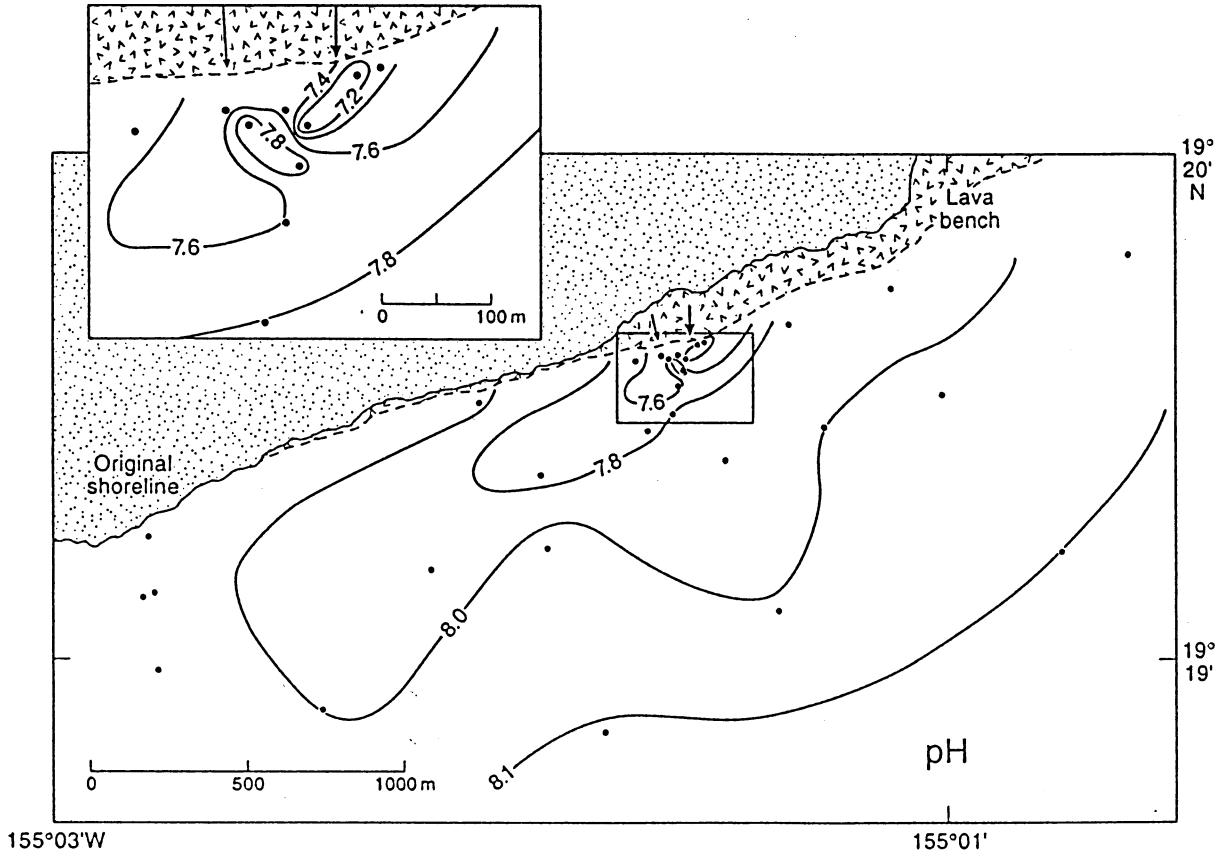

Fig. 1. pH offshore of Wahaula where lava entered the ocean on March 1, 1991 (See location map, Sansone and Resing 1995). Filled circles represent sampling locations and arrows show locations of the lava entries on this date.

ionic strength as well as the same amount of [Cl^-]. To each of these solutions $NaHCO_3$ was added. The $NaHCO_3$, when dissolved, adds a known alkalinity to the samples, which then gets titrated by acid added generated in the experiment. By measuring the alkalinity before and after the experiment the exact amount of acid generated can be established. Samples were filtered within 10 to 30 min of the completion of each experiment. The lava on this day was viscous and slow moving.

4.1.3.5. October 13, 1995 (October DIW). Five experiments were conducted with lavas from a broad flow front >100 m across. Single blobs of lava were added to known volumes of DIW. The lava at this site was fluid and fast moving. Samples were filtered within 10 to 30 min of the completion of each experiment.

4.2. Analytical

For the DIW experiments, Na^+, Fe^{3+}, Ca^{2+}, Mg^{2+}, and Sr^{2+} were determined by inductively coupled plasma atomic emission spectrometry (ICP-AES) and Al^{3+} was determined by flow injection analysis (Resing and Measures, 1994). Na^+, Fe^{3+}, Sr^{2+}, and Al^{3+} in the precipitation samples were also determined by ICP-AES. Potassium in samples of precipitation and from the DIW experiments was determined by flame AES. Total alkaline earth concentrations (±0.05%) for the surface ocean seawater and precipitation samples were determined by titration (e.g., Geiskes and Peretsman, 1986) with automated spectrophotometric end point detection. Mg^{2+} (±0.1%) was calculated as the total alkaline earth concentration less Ca^{2+} and Sr^{2+}. Ca^{2+} (±0.1%) for surface ocean samples and precipitation samples was determined by titration with automated end point detection using a Ca^{2+} electrode (Whitefield et al., 1969).

Chlorinity (±0.05%) in the surface ocean and precipitation samples was determined by titration with 0.1 mol L $AgNO_3$. Chloride (±10%) was determined in the DIW experiments by ion chromatography (IC). Sulfate (±1%) for all samples was determined using IC. Fluoride (±3%) for all samples was determined using a fluoride-sensitive electrode (Warner, 1971; Froelich et al., 1983).

pH was measured by using a combination pH electrode. Because of CO_2 degassing from the samples, pH determinations for surface ocean samples were generally made as soon as possible after collection. pH for the DIW experiments was measured in the laboratory by adding KCl or NaCl to the samples as an ionic strength adjuster; H^+ activity was determined using pH and was converted to [H^+] using the Davies equation (Langmuir, 1997). Alkalinity was determined by titration by a modification of the method of Edmond (1970). The acidity of the precipitation samples was measured by pipetting a known volume of sample into a seawater sample of known alkalinity, followed immediately by the alkalinity titration discussed above. Acidity was the difference between the known alkalinity of the seawater and the subsequent alkalinity after the addition of the precipitation sample. Total dissolved inorganic carbon (ΣCO_2) was measured (±1.0%) by gas chromatography (Weiss and Craig, 1973).

5. RESULTS

5.1. Sea Surface

Where the lava flows into the ocean at the shoreline of Kilauea Volcano there is a large pool of heated water (see Sansone and Resing, 1995) with pH values below that of the surrounding seawater (Fig. 1). In addition to the decrease in pH, there are decreases in alkalinity and ΣCO_2, and all three decreases correlate well with water temperature (Fig. 2). The decrease in pH, together with the decrease in alkalinity, show that there was an addition of acid to the seawater at the lava entry and not an addition of magmatic CO_2 as seen at other submarine eruptions (e.g., Cheminée et al., 1991; Duennebier et al., 1997). The decrease in ΣCO_2 suggests that the carbonate alkalinity in the local seawater is titrated by the acid and is converted to CO_2, and this CO_2 then must escape to the atmosphere.

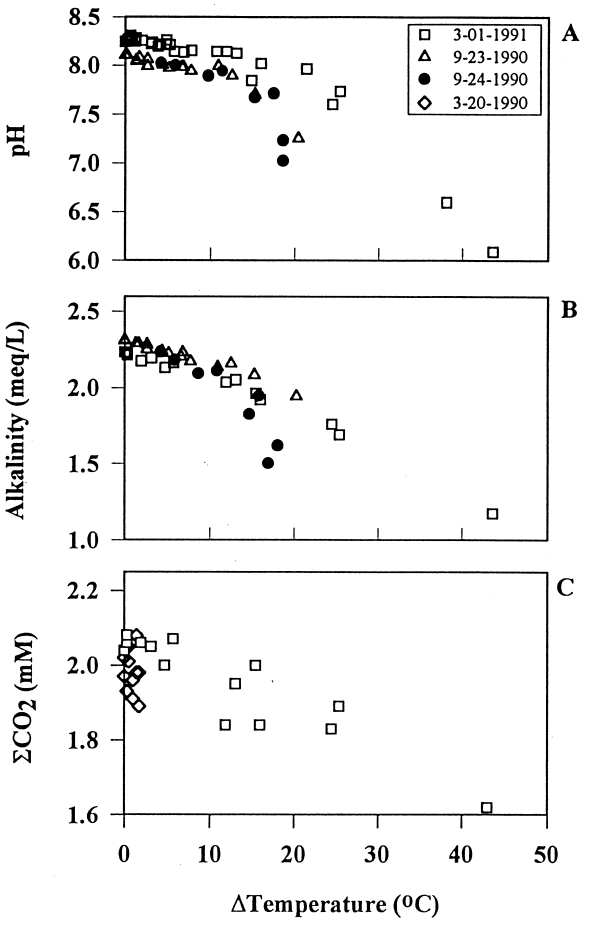

Fig. 2. (A) pH, (B) alkalinity, and (C) ΣCO_2 versus change in temperature (relative to local seawater) of seawater collected offshore of the lava entries (for locations, see Sansone and Resing, 1995).

5.2. Precipitation

The most striking features of the precipitation samples are their elevated acidities and chlorinities. The samples ranged in pH from 1.1 to 2.1 and chlorinities ranged from 1.7 to 3.7 times the chlorinity of the local seawater (Table 3). The acidity in the precipitation samples was great enough to make H^+ a major cation in the solution. The major ions in the precipitation samples are accounted for by H^+, Na^+, Cl^-, Mg^{2+}, SO_4^{2-}, Ca^{2+}, K^+, Fe^{3+}, Al^{3+}, and Sr^{2+}. The elemental enrichments increase in proportion to Cl^- content, as shown for Na^+, Mg^{2+}, SO_4^{2-}, and Ca^{2+} in Figure 3, where the lines are the ratios of the given elements to [Cl^-] in local seawater. As can be seen, the concentrations of these elements are of a similar ratio to Cl^- in the precipitation as they are in the local seawater. In Table 4 the ratios of the different elements to Cl^- are shown along with the ratio ordinarily found in seawater. The ratios in the precipitation samples show depletions in Sr^{2+}, K^+, Mg^{2+}, and Na^+ and enrichments in Li^+, SO_4^{2-}, F^-, Al^{3+}, and Fe^{3+}. In addition, HCO_3^- and CO_3^{2-} are completely absent at the pH values of these solutions. A charge balance of the major ions shows that no other major ions are unaccounted for in solution (Table 3). Samples 91-6 and 91-7 show a larger

Table 3. Major elemental components of precipitation samples and local seawater (in mmol/kg except for pH).

	91-6	91-7	95-16	95-1	95-2	95-3	SW
Cations							
pH	2.07	2.12	1.22	1.09	1.32	1.51	8.10
H^+	10.0	8.4	62.2	57.2	35.9	28.4	−2.2
ΣH^+*	18.6	19.4	78.3	76.6	53.7	42.5	
Na^+	776	747	1409	1585	1479	1209	463
Na^+ (Ch. Bal.†)	752	723	1422	1622	1460	1233	
% Diff‡	3.2%	3.2%	0.9%	2.3%	1.3%	2.0%	
K^+	17.4	16.0	30.4	34.0	30.9	26.3	10.1
Mg^{2+}	86.1	82.5	162.8	184.1	167.5	139.8	52.7
Ca^{2+}	17.8	17.0	31.3	35.9	30.0	27.6	10.2
Fe^{3+}	0.64	0.94	1.07	1.41	1.32	1.01	0.00
Al^{3+}	1.01	1.55	1.93	2.39	2.24	1.66	0.00
Sr^{2+}	0.14	0.14	0.26	0.29	0.24	0.22	0.09
Anions							
Cl^-	889	853	1721	1944	1742	1460	540
Br^-§	1.4	1.3	2.7	3.0	2.7	2.3	0.8
F^-	0.44	0.43	2.72	2.12	2.06	1.50	0.07
SO_4^{2-}	51.0	50.0	92.8	108.0	92.7	83.5	27.9
Charge balance							
Σz^+	1017	978	1899	2128	1952	1607	597
Σz^-	993	954	1912	2165	1932	1631	597
$(\Sigma z^+ - \Sigma z^-)$	25.5	23.6	−12.8	−36.6	19.7	−23.9	0.1
% Difference	2.4%	2.4%	−0.7%	−1.7%	1.1%	−1.5%	0.0%

* $\Sigma H^+ = [H^+] + (\text{alkalinity} \times (Cl_p^-/Cl_{SW}^-)) + (3Fe^{3+}) + (3Al^{3+})$.
† Na by charge balance.
‡ % Difference between measured Na and Na calculated by charge balance.
§ Br^- assumed to be conservative and calculated based on Cl concentration.

imbalance than the other samples. We suspect that this may arise from the fact that Na^+ was measured 4 years after Cl^-, and evaporation probably resulted in elevated Na^+ concentrations in these samples.

In general, the ratios of the major ions to Cl^- are similar to those in seawater, suggesting that seawater is the primary source of these ions. Therefore, these fluids primarily reflect the evaporation of water from seawater, spatter from phreatic explosions, or the condensation of vapor and its aggregation onto glassy and salty particles and droplets. In contrast, the source of the F^-, Fe^{3+}, Al^{3+}, and some of the S must be the lava.

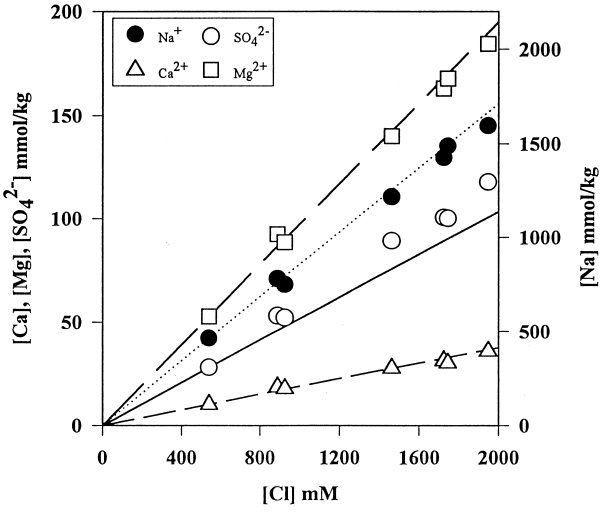

Fig. 3. Major elements in precipitation samples versus Cl^-. The lines represent the element:Cl^- ratio found in seawater.

To account for all of the acid produced in forming the precipitation samples, we must account for the measured H^+ ion concentration, the acid used to titrate the alkalinity of the seawater, and the acid used to liberate cations from the basalt into the water. This can be calculated as follows:

$$\Sigma H^+ = [H^+] + (\text{alkalinity}_{sw} \times (Cl_p^-/Cl_{sw}^-)) + (3Fe^{3+}) + (3Al^{3+}) \quad (8)$$

where the term $[\text{alkalinity}_{sw} \times (Cl_p^-/Cl_{sw}^-)]$ is an estimate of the alkalinity that would be associated with seawater of higher chlorinities.

Table 4. Ratios of major elements to Cl^- for precipitation samples.

	Average (X:Cl^-) of six samples	R^2*	(X:Cl^-) of seawater	% of seawater†
Sr	$1.51 \pm 0.09 \times 10^{-4}$	1.00	1.67×10^{-4}	90%
K	$1.83 \pm 0.07 \times 10^{-2}$	1.00	1.87×10^{-2}	98%
Mg	$9.60 \pm 0.09 \times 10^{-2}$	1.00	9.75×10^{-2}	98%
Na	$8.43 \pm 0.24 \times 10^{-1}$	1.00	8.58×10^{-1}	98%
Ca	$1.88 \pm 0.10 \times 10^{-2}$	0.99	1.88×10^{-2}	100%
Li	$4.70 \pm 0.15 \times 10^{-5}$	1.00	4.63×10^{-5}	102%
S	$5.60 \pm 0.19 \times 10^{-2}$	0.99	5.17×10^{-5}	108%
F	$9.81 \pm 3.80 \times 10^{-4}$	0.91	1.22×10^{-4}	800%
Al	$1.10 \pm 0.25 \times 10^{-4}$	0.85	9.26×10^{-8}	1.2×10^{6}%
Fe	$6.59 \pm 1.54 \times 10^{-3}$	0.82	1.85×10^{-9}	3.6×10^{7}%

* R^2 is the correlation coefficient of each element regressed against Cl^-.
† {Average (X:Cl^-)}/{Seawater(X:Cl^-)} × 100%.

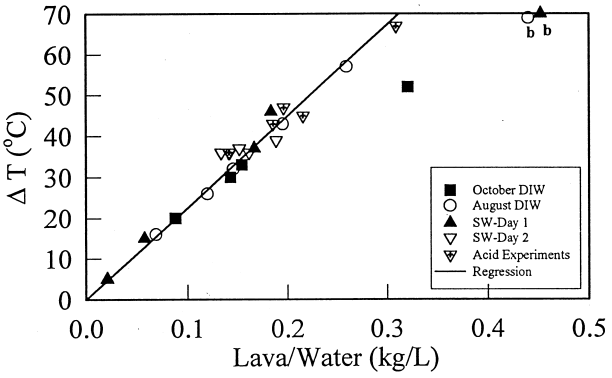

Fig. 4. The change in water temperature versus amount of lava added (kg/L). The letter "b" indicates a sample that boiled. The line is a least squares linear regression through points not labeled with b (slope = 221°C/(kg/L); R^2 = 0.94).

5.3. Experiments

In each of the experiments conducted here, the addition of lava to the water caused an immediate and intense reaction in which the surface of the lava was coated with many small (~2–5 mm) steam bubbles, whereas larger steam bubbles (~5 to ~30 mm) were emitted at or generated from cracks and holes on the surface. The morphology of these samples resembled that of the "floating rocks" found in the surface ocean (Sansone and Resing, 1995; Resing, 1997), although the samples had vesicles (<1 to ~20 mm), which were somewhat smaller than those found in the floating rocks. During the reaction, the vesicles filled with steam and the lava often floated until its temperature equilibrated with that of the water, at which point the vesicles filled with water and the lava sank to the bottom of the sample container. The quenched glass was shiny and, despite its friable nature, stayed together as a single piece. The bottom of the experimental containers were covered with translucent golden-brown glass that closely resembled the glass found suspended in the surface oceans (Resing, 1997). Although small opaque pieces of the lava were also present in the containers, there was no apparent formation of black sand (black sand is uniformly sized shattered glass found as beaches and as a part of underwater talus deposits near the ocean entries).

In each of the experiments performed, water temperature increased in direct proportion to the amount of lava added (Fig. 4). Elemental enrichments were also proportional to the amount of lava added as shown in Figures 5 and 6 for the major elements in solution in the DIW experiments. In addition, enrichments that correlated with temperature were observed in both the seawater and DIW experiments for many trace elements (Resing, 1997; J. A. Resing and F. J. Sansone, in prep.). In all of the experiments acid (H^+) was generated when lava was placed in contact with water. The acidity generated in the seawater experiments (as reflected in the decrease in alkalinity), when plotted versus the change in water temperature, closely matches that observed in the surface ocean (Fig. 7). The amount of acid generated in the DIW experiments is proportional to the change in temperature of the water and to the mass of lava added (Fig. 8A), although the acidity generated in DIW

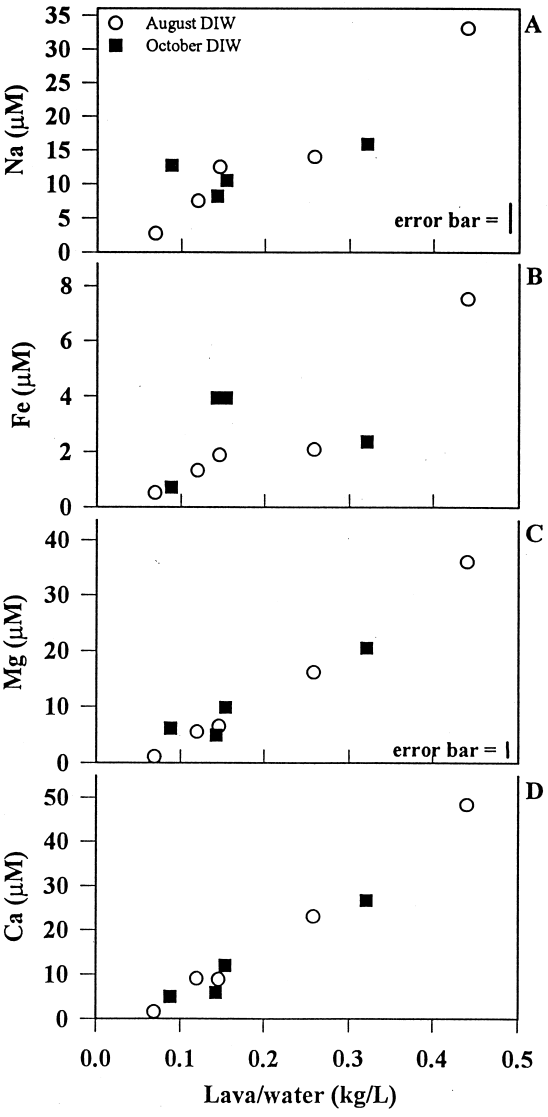

Fig. 5. Major ion elemental enrichments for Na^+ (A), Fe^{3+} (B), Mg^{2+} (C), and Ca^{2+} (D), versus lava water ratios in DIW experiments. The error bars represents the analytical precision of the measurements where error is greater than symbol size.

experiments was considerably less than that in the seawater. In the DIW experiments H^+ is the major cation in solution (Table 5), and the anions are almost entirely accounted for by SO_4^{2-} and F^-, with a small contribution from Cl^-. In one DIW experiment the water came to a rapid boil, which lasted several minutes. In this experiment [H^+] was much lower than expected (Fig. 8A) but, because the total cations released to solution versus lava/water show a continuous increase (Fig. 8B), this depletion must reflect the exchange of H^+ for other cations during reaction with the basalt.

In the experiments designed to identify the water–lava reactions responsible for the generation of acidity, it was observed that the solutions containing both Mg^{2+} and Na^+ did not generate acidity in excess of those solutions containing Na^+ but no Mg^{2+} (see Table 2). In each of the experiments where Na^+ was present at its seawater concentration, acidity was

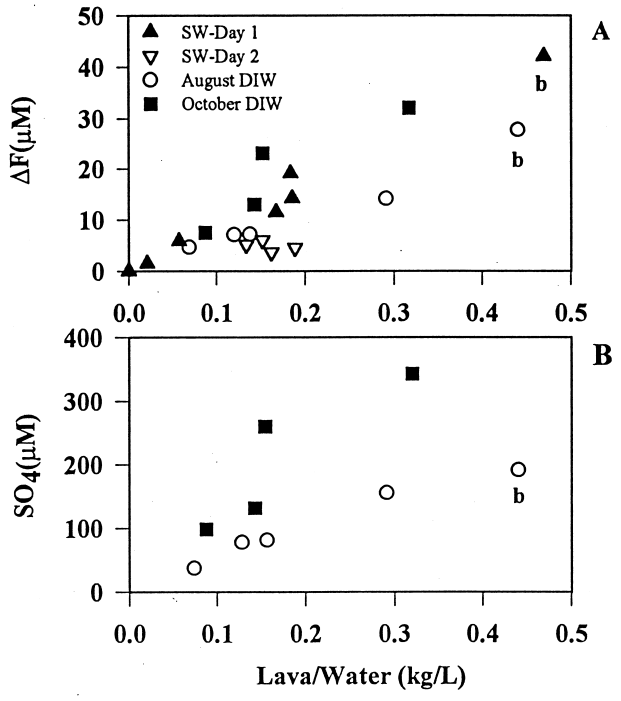

Fig. 6. Elemental enrichments for F^- (A) and SO_4^{2-} (B) versus concentration of lava added.

generated at levels similar to that observed for seawater. These experiments suggest that Na-metasomatism as opposed to Mg-metasomatism is the primary water–lava reaction responsible for the generation of acidity during lava–water contact.

6. DISCUSSION

6.1. General

An evaluation of the results indicates that the generation of acidity during lava–seawater contact arises from two sources, magmatic volatiles and water–rock reactions. The data suggest that the primary magmatic volatile is S and the primary water–rock reaction is Na-metasomatism.

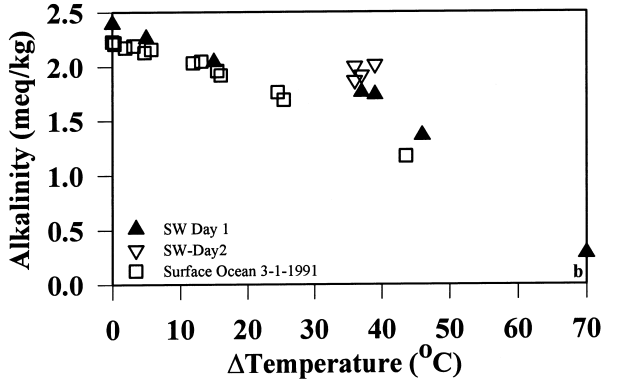

Fig. 7. The generation of acidity in surface ocean samples and from lava–water experiments. The generation of acidity is manifested by a decrease in alkalinity. The letter "b" indicates a sample that boiled.

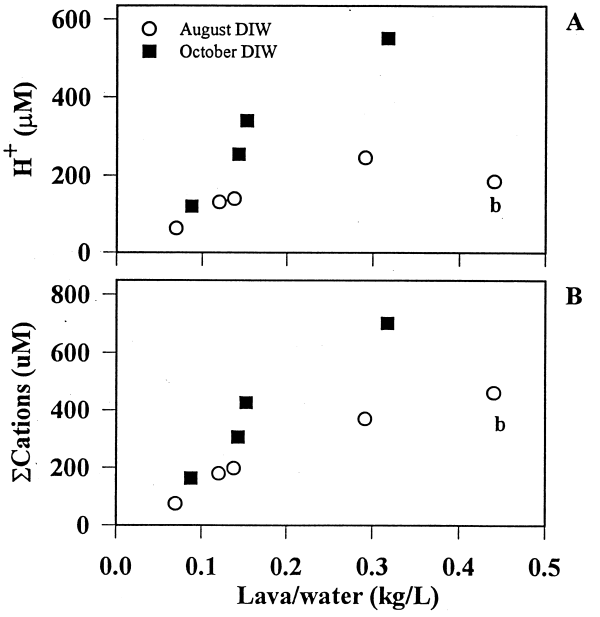

Fig. 8. (A) Total acid versus concentration of lava in the DIW experiments. (B) Total cations in solution versus concentration of lava in the DIW experiments. The letter "b" indicates a sample that boiled.

In the arguments presented below, increases in acidity from magmatic S and F increase the concentrations in SO_4^{2-} and F^- found in the aqueous phases discussed. We assume that excess magmatic S as SO_2, H_2S, and S_2 produces $2H^+$ (Eqns. 2–5) and excess F^- as HF produces $1H^+$ (Eqn. 6). As shown for Mg^{2+} in Eqn. 2, acidity generated from seawater–lava reactions removes Na^+, Ca^{2+}, and/or Mg^{2+} from the aqueous phase to the solid phase, with decreases in the concentrations of Na^+, Ca^{2+}, and Mg^{2+} resulting in the production of $1H^+$, $2H^+$, and $2H^+$, respectively. Thus, to identify the sources of acid, we examine the changes in the concentrations of these major ions in our samples.

6.2. Surface Seawater

Identifying the sources of acid in the surface ocean seawater is difficult because the water altered during the interaction with the lava is diluted by ambient seawater before being sampled. As a result, observing the addition of acid as either a depletion in one of the major cations or as an increase in a major anion is obscured by the high concentrations of dissolved salts in seawater. The maximum observed decrease in alkalinity in the surface ocean samples was ~1 mEq (Fig. 2B).

The addition of 1 mmol/L of acid would be reflected in the addition of acidic anions and/or the removal of seawater cations. If all of the acid was formed from the removal of 0.5 mmol/L Ca^{2+} or Mg^{2+} from solution, it would represent ~5% of the Ca^{2+} or ~1% of the Mg^{2+} originally present in the ambient seawater. These changes can be resolved by the 0.1% precision of the techniques used to measure Ca^{2+} and Mg^{2+}. Figures 9A and 9B show that $[Ca^{2+}]$ and $[Mg^{2+}]$ increase (as opposed to a decrease) in concentration as a function of temperature for the March 1, 1991, samples, suggesting that neither is responsible for acid formation. When normalized to chloride

Table 5. Concentrations of major elements in the DIW experiments.

	Concentrations (μmol/L)									
	802	807	809	810	814	1007*	1008	1009	1010	Average
Cations										
Na^+	12.5	7.5	33.1	14.0	2.7	12.7	15.9	8.2	12.5	
Ca^{2+}	8.9	9.0	48.4	23.0	1.6	5.0	26.7	5.9	11.9	
Mg^{2+}	6.5	5.6	36.0	16.2	1.1	6.2	20.6	4.9	9.9	
Fe^{3+}	1.88	1.32	7.52	2.08	0.52	0.72	2.37	3.94	3.94	
K^+	—	—	—	—	—	0.97	1.33	0.92	1.41	
Al^{3+}	3.2	2.7	17.8	8.5	0.8	2.0	10.7	3.1	6.4	
H^+	139	130	185	246	63	119	551	255	340	
$\%H^{+\dagger}$	70%	73%	40%	66%	84%	73%	79%	83%	80%	72 ± 13%
Anions										
SO_4^{2-}	82	78	192	156	37	98	343	132	260	
Cl^-	2	0	7	0	1	15.6	5	8.5	6.8	
F^-	7.26	7.11	27.81	14.15	4.69	7.49	32.05	12.96	23.12	
$S:F^{\ddagger}$	11.2	11.0	6.9	11.0	8.0	13.2	10.7	10.2	11.2	10.4 ± 1.8
Charge balance										
ΣZ^-	172	163	419	327	80	220	723	285	550	
ΣZ^+	198	179	463	370	75	163	702	307	427	
% Diff§	14%	9%	10%	12%	−7%	−30%	−3%	7%	−25%	

* Contaminated with SW.
† $H^+/Z^+ \times 100\%$.
‡ SO_4^{2-}/F^-.
§ $(\Sigma Z^+ - \Sigma Z^-)/(\Sigma Z^+ + \Sigma Z^-) \times 2 \times 100\%$.
— data not available.

or salinity, Ca^{2+} and Mg^{2+} concentrations are seen to be nearly constant relative to the ambient seawater (Fig. 9). The increases in Ca^{2+} and Mg^{2+}, therefore, reflect water vapor loss during steam formation. If, instead, the acid came from the uptake of Na^+ by the basalt, the 1 mmol/L loss in Na^+ from a solution originally containing 460 mmol/L Na^+ would represent a 0.2% loss. This loss would be imperceptible given the 1.5% precision of the method of determination for Na^+.

Measurements of sulfate in the surface ocean waters showed no discernable increase. If all the acidity resulted from the addition of magmatic S, then we would expect a 1 mmol/L increase in SO_4^{2-} versus a background concentration of ~28 mmol/L; this would be a 3.6% increase, which would be barely resolvable versus the 1% precision of determination. In contrast, an enrichment in F^- is clearly discernable in the surface ocean and correlates well with water temperature (Fig. 9C). The largest addition of F is ~30 μmol/L, which if added as HF, represents <3% of the total acid added to these solutions. If we assume that the altered waters in the surface ocean had a similar ratio of S:F delivered to them as in the DIW experiments (Table 5), we can then make an estimate of the contribution of S gasses to the surface ocean. The average S:F ratio in the nine DIW experiments was 10.4 ± 1.7:1 (Table 5); therefore $\Delta SO_4^{2-} = \Delta F^- \times 10.4$, yielding a maximal $\Delta SO_4^{2-} \approx 310$ μmol/L, which is an ~1% increase over background SO_4^{2-}, an increase that would be indistinguishable from the background seawater for our method of detection.

By combining the known ΔF^- with the calculated ΔSO_4^{2-} we can estimate the contribution that magmatic gasses make to the total acid added to the surface ocean. We calculate this value for March 1, 1991, using samples with $\Delta F^- > 1$ μmol/L (Fig. 9C), and estimate that magmatic gasses are responsible for 32 ± 6% of the acid added to the surface ocean on this date.

The lava–seawater contact causes a large decrease in pH, alkalinity, and ΣCO_2 in the surface ocean. The F^- enrichment shows that some of the acid comes from acidic magmatic gasses. The invariant Mg^{2+} and Ca^{2+} concentrations suggest that the acidity must not have been generated to any great extent from Ca- or Mg-metasomatism. These results suggest that there must be another process responsible for the balance of the acid generation.

6.3. Precipitation

The precipitation samples had a greater amount of acid added to them than did the surface seawater. This results in H^+ being a major ion in these solutions, with concentrations ranging from 8 to 62 mmol/L (Table 3). To assess the relative enrichments and depletions for the different elements in the precipitation, we normalize their concentrations using Cl^-. Cl^- is appropriate for normalization because it can be determined very accurately and is believed conservative in this setting. Data on gasses from Kilauea show that Cl^- and F^- concentrations are similar in the magmatic gasses at the summit of Kilauea (Greenland, 1984; Miller et al., 1990). In addition, basalts from Kilauea have $[F] \cong 8 \times [Cl]$ (Govindaraju, 1989). The most F^--rich precipitation sample was 2.71 mmol/L F^- and in the DIW experiments $[Cl^-] \ll [F^-]$ (Table 5). This suggests that the lava must contribute ≪2.7 mmol/L Cl^- to the precipitation. If F and Cl flux from the lava were equal, then the 2.7 mmol/L of magmatic Cl^- would only represent <0.14% of the ΣCl^- and would be indistinguishable from seawater Cl^- using our methods of determination. Using $[Cl^-]$ of the precipitation and the ratio of the ions in seawater to $[Cl^-]$ in seawater we can estimate the contributions of the major elements in the precipitation that came from seawater $[X_{SW}]$. The difference between the measured concentration of an element, $[X_p]$, and $[X_{SW}]$ is the amount by which the precipitation has

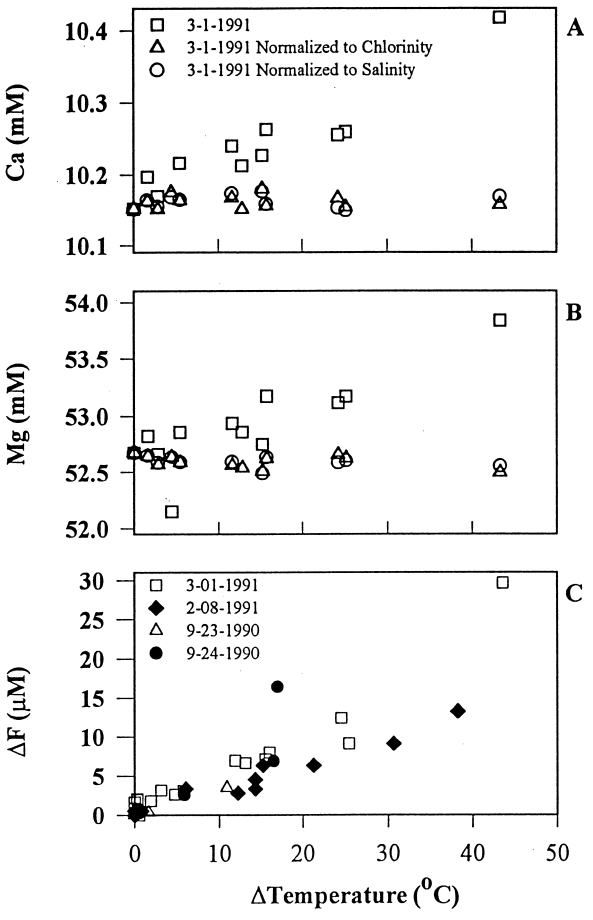

Fig. 9. Elemental enrichments versus change in temperature of seawater samples collected offshore of the lava entries. (A) Ca^{2+}, (B) Mg^{2+}, and (C) ΔF^-. Ca^{2+} and Mg^{2+} are normalized to chlorinity or salinity as follows: $[X_n] = [Cl^-_{BSW}] \times [X_s] \div [Cl^-_s]$ where $[X_s]$ is the concentration of element X in a sample and $[Cl^-_{BSW}]$ and $[Cl^-_s]$ are the chloride (or salinity) in background seawater and a sample, respectively.

been altered by some process other than evaporation and will be called the excess of element X or $[X_{ex}]$:

$$[X_{ex}] = [X_p] - [X_{SW}] \quad (9)$$

In these calculations, depletions in X are negative and enrichments are positive. Enrichments are observed for S and F while depletions are observed for many of the cations. Converting these depletions and enrichments into contributions to acidity (Table 6) shows that enrichments in SO_4^{2-} and F^- from magmatic gasses contribute 34 ± 20% of the acidity present in the samples. The contribution to acidity from Mg-metasomatism is 6 ± 4% and that from Ca^{2+} and K^+ is relatively small. The data show that the bulk of the acid was created by Na-metasomatism (56 ± 9%).

6.4. Experiments

The amount of acid generated in the seawater experiments is greater than that in the DIW experiments, with 4.0 ± 1.5 mEq of acid generated per kilogram of lava added to the seawater experiments and 1.0 ± 0.5 mEq of acid generated per kilogram of lava added to the DIW experiments (Table 7). These results clearly implicate two different sources of acidity. The first is independent of the initial composition of the water and implicates the lava as its sole source. SO_4^{2-} and F^- correlate well with the concentration of lava in the experiments (Fig. 6) and are the two major anions found in the DIW experiments (Table 5), suggesting that the S- and F-rich magmatic gasses escaped the molten lava into solution. The second mechanism indicates that the components present in seawater must react with the lava to generate acidity. In Table 2 we see that, where NaCl is present, acid is generated in great excess to that expected solely from S and F gasses. In the three experiments where Mg^{2+} was present at seawater concentrations, acidity generated was 5.7, 2.3, and 2.2 mEq per kilogram of lava. In the experiment where 5.7 mEq of acid was created, the water in the experiment boiled vigorously for ~3 min. The formation of "extra" acid might have been the result of increased water and steam circulation through the lava, or it may have been associated with the increased reaction time at the temperature of reaction. Nonetheless, acid generation in the NaCl solutions is equal to that generated in solutions containing Mg^{2+} and Na^+ at seawater levels. Therefore, these data show that Mg^{2+} does not appear to enhance the formation of acid and Na^+ is the most important cation being hydrolyzed.

The division between the two sources of acid can be evaluated most directly from the NaCl and $MgCl_2$ experiments,

Table 6. Quantification of acid sources from "excess" values.

	Magmatic gas generated			Water–rock generated						
	$[F^-]_{ex} \times 1$	$[SO_4^{2-}]_{ex} \times 2$	ΣH^+_g	$[Mg^{2+}]_{ex} \times -2$	$[Ca^{2+}]_{ex} \times -2$	$[K^+]_{ex} \times -1$	$[Na^+]_{ex} \times -1$	ΣH^+_{w-r}	ΣH^+_{ex}	Expected ΣH^+
91-6	0.33	10.0	10.3	1.3	−2.1	−0.7	10.1	8.5	18.8	18.6
91-7	0.33	11.7	12.1	1.0	−2.0	−0.1	8.4	7.3	19.4	19.4
95-16	2.51	7.5	10.0	10.2	2.1	1.8	54.2	68.3	78.3	78.3
95-1	1.89	15.0	16.9	11.0	1.3	2.4	45.1	59.8	76.7	76.6
95-2	1.85	5.2	7.0	4.9	5.5	1.7	34.7	46.8	53.9	53.7
95-3	1.32	16.0	17.3	5.2	−0.3	1.0	19.3	25.3	42.6	42.5

$\Sigma H^+_g = 2 \times [SO_4^{2-}]_{ex} + [F^-]_{ex}$.
$\Sigma H^+_{w-r} = -2 \times [Mg^{2+}]_{ex} - 2 \times [Ca^{2+}]_{ex} - [K^+]_{ex} - [Na^+]_{ex}$.
$\Sigma H^+_{ex} = \Sigma H^+_{w-r} + \Sigma H^+_g$.
$\Sigma H^+ = [H^+] + (\text{alkalinity} \times (Cl^-_p/Cl^-_{sw})) + (3Fe^{3+}) + (3Al^{3+})$ (Eqn. 2).
ΣH^+_g and ΣH^+_{w-r} are total contributions to acidity from gasses and water–rock reactions, respectively.

which initially contained Na^+ and/or Mg^{2+} at seawater levels but contained no SO_4^{2-} (Table 2). Upon completion, the SO_4^{2-} in these experiments was 0.093 mmol/L (0.186 mEq H^+) for the NaCl experiment and 0.318 mmol L for the $MgCl_2$ experiment (0.636 mEq H^+). This represents 40% and 32% of the acidity generated for these two experiments, respectively. Furthermore, if it is assumed that S present in the DIW experiments is representative of that present in the seawater experiments, then this S represents 14 to 40% of the total acid created when lava comes in contact with seawater. When F^- is included, 16 to 45% (average 25%) of the acid comes from magmatic gas with the remainder coming from water–rock reactions.

6.5. Magmatic Volatiles

The concentrations of S and F that remain in the lava after its initial degassing are approximately the same. However, the ratio of S:F found in the water in the DIW experiments (10.4 ± 1.8) demonstrates that S is more easily degassed than is F. The amount of S found in the DIW experiments represents ~10 to 38% of the residual S (Cashman et al., 1994) in the lava, whereas the amount of F is <0.5% of the residual F (Greenland et al., 1985) in the lava. The lava sampling technique used by Cashman et al. (1994) was to quench molten lava samples in water (K. V. Cashman, pers. comm.), suggesting that they may have underdetermined their S concentrations by 10 to 38%.

The results presented here show that S and F were responsible for ~30% of the acidity generated where degassed lava enters the ocean at Kilauea Volcano. When erupted beneath the sea at higher pressures, the lava retains most of its volatiles (Meunow et al., 1979; Wallace and Carmichael, 1992) and acidity from this source during eruption decreases in importance. As the eruptions become shallower the gasses are more likely to be released. The gasses can separate from the magma either in the magma chamber before eruption or can separate from the magma as it ascends and erupts. In addition, we have shown here that upon contact with seawater a portion of the magmatic gasses that is dissolved in the lava can be released. As mentioned above, the lava placed into water in the experiments stayed together as a single blob with many large internal vesicles. This implies that violent phreatomagmatic eruptions that create fine hyaloclastic materials are not required to release a significant portion of the residual volatiles from the basalt. Although, the accumulation of S on the rims of pillow basalts at depths of >4000 m at Kilauea (Meunow et al., 1979) suggests that there is a mechanism by which the S migrates out of the basalt as it freezes, and thus it should be expected that the greater the amount of glass exposed to seawater through violent phreatomagmatic eruptions, the greater the release of gasses. The more explosive eruptions are thought to occur in maximum water depths of 1 km, and more frequently at depths <500 m (Kokelar, 1986; Cas, 1992). However, observations made at other submarine eruptions at greater depths and pressures show that the magmatic volatile CO_2 escapes from magmas during submarine eruptions (Cheminée et al., 1991; Duennebier et al., 1997). Although the higher pressures present at submarine eruptions may make partitioning of S, F, and Cl into the solid phase more likely, the CO_2 may act as a carrier phase for these elements (Gerlach, 1993) and thus the release of CO_2 may promote the release of S, F, and Cl, along with other volatile elements.

6.6. Water–Rock Reactions

As discussed above, the predominant acid-forming reaction in oceanic hydrothermal systems is Mg-metasomatism. Mg-metasomatism was also proposed for lava–seawater contact by Gerlach et al. (1989), who suggested the mechanism was a dry steam reaction in which $Mg(OH)_2$ was formed and HCl escaped into the gas phase. Ca-hydrolysis reactions similar to that proposed by Gerlach et al. (1989) have been shown to take place in solutions of $CaCl_2$ in which boiling takes place at temperature and pressure ranges of 380°C and ≤230 bars to 500°C and ≤580 bars (Bischoff et al., 1996). Our results demonstrate, however, that Na-metasomatism is most responsible for forming the acid observed here. The small amount of Na-rich solid material that was created here makes identification of a specific sodic phase difficult, and therefore, we are left to speculate as to its composition and the mechanism by which Na^+ uptake is achieved.

The reactions at the lava–seawater interface observed here took place at 1 bar pressure and an unknown temperature, suggesting that the phases present might include liquid and solid basalt, liquid and vaporous water, and aqueous-, solid-, and liquid-phase NaCl. The generation of $HCl_{(g)}$ through the hydrolysis of Na^+ when NaCl is in contact with water vapor at high temperatures (>450°C) and low pressures is a well-described phenomenon (Hanf and Sole, 1970; Galobardes et al., 1981; Armellini and Tester, 1993; Fournier and Thompson, 1993). The reaction was shown to be:

$$NaCl_{(s,l)} + H_2O_{(g)} \rightarrow NaOH_{(s)} + HCl_{(g)} \quad (10)$$

where the $HCl_{(g)}$ escapes due to its preference for the gas phase. However, in systems where the HCl is allowed to condense and come in contact with the NaOH, the reaction reverses itself and goes unnoticed. The addition of SiO_2 to this reaction system markedly increases the yield of HCl due to the formation of a Na–silicate phase (Clews and Thompson, 1922; Fournier and Thompson, 1993):

$$2NaCl_{(s,l)} + 2SiO_{2(s,l)} + H_2O_{(g)} \rightarrow Na_2Si_2O_{5(s)} + 2HCl_{(g)} \quad (11)$$

Na–silicate phases like the one produced in Eqn. 11 show retrograde solubility (Rowe et al., 1967) and, although relatively insoluble above 300°C, are completely soluble below 100°C (Weast, 1970). The observations made here suggest a final product that is not readily soluble in water. If the reaction product was soluble, its dissolution would generate a basic solution. In the experiments this base would have neutralized the acid. Where the lava flows into the ocean, the HCl would be partitioned into the gas phase, leaving the resultant base in contact with the surface ocean, raising the pH of this water. Because we observed a decrease in pH in the surface ocean and in the experiments, the reaction product must not be readily soluble, suggesting that the lava–seawater reactions produce neither NaOH nor a simple Na–silicate. Instead, the final product created during this reaction must be largely insoluble.

Clews and Thompson (1922) point out that the generation of HCl at high temperatures was much more vigorous in the

presence of an aluminosilicate phase. Fournier and Thompson (1993) suggest that in nature Na–silicate is not likely to form but that "it is likely that salt and quartz would react with various aluminum-rich silicates, forming alkali feldspars and other common hydrothermal products." Consider the following general reaction:

$$6SiO_{2(s,l)} + Al_2O_{3(s,l)} + 2NaCl_{(s,l)} + H_2O_{(g,l)} \rightarrow 2NaAlSi_3O_8 + 2HCl_{(g)} \quad (12)$$

where SiO_2 and Al_2O_3 are components of the basaltic glass. In this case, albite is formed, but this does not preclude the formation of Na-rich smectites or other feldspars. Although the other cations participate in this reaction, Na^+ may be used preferentially over Mg^{2+} and Ca^{2+} due to its 9- and 45-fold enrichment over the latter elements in seawater. The ratio of acid formed from Na^+ to that formed by Mg^{2+} is 6.0 ± 1.7, which is close to the ratio of Na:Mg found in seawater (8.8).

Another possible reaction mechanism is the high-temperature hydrolysis of the glass substrate (e.g., Rimstidt and Barnes, 1980) followed by the exchange of seawater cations with hydrogen ions at the silicate surface. The dissolution of Si from the glass surface occurs through the complete hydrolysis of SiO_2 to form $Si(OH)_{4(aq)}$. Incomplete hydrolysis of the SiO_2, however, may leave the Si at the glass surface partially hydrolyzed [e.g., $SiO(OH)_2$]. At this stage, H^+ could exchange for cations from the seawater. The elevated concentrations of dissolved Si and Al observed in the precipitation samples and the relatively short contact time between the seawater and the lava indicate that the silicate hydrolysis must have happened very quickly. It has been noted that the speed of silicate hydrolysis is proportional to temperature (Rimstidt and Barnes, 1980; Tester et al., 1994) suggesting that the hydrolysis of the basalt surface took place at high temperatures. In addition, Dove and Crerar (1990) noted that the presence of cations in solution enhance the Si-hydrolyzation process through the adsorption of the cations onto the silicate surface. Their data show that Na^+ and K^+ are more readily adsorbed onto these sites than is Mg^{2+}, which is consistent with the results observed here. The reaction product from this process would also be an Al–silicate phase, most likely a Na-rich smectite.

The experimental results of Fournier and Thompson (1993) show that the formation of $HCl_{(g)}$ by Na-hydrolysis is inversely proportional to pressure, which agrees well with stoichiometric considerations whereby $HCl_{(g)}$ formation should be inversely proportional to the square root of pressure (M. E. Berndt, pers. comm.). However, the data of Fournier and Thompson (1993) showed that HCl was formed at pressures >250 bar at 600°C by the reaction shown in Eqn. 10, and at pressures >300 bar and 600°C when SiO_2 was present as in Eqn. 11. Na-metasomatism has also been shown to occur in Mg-replete hydrothermal fluids leading to the formation of albitic plagioclase (Seyfried and Janecky, 1985; Berndt et al., 1989). During the reaction of basaltic glass with solutions of NaCl, $CaCl_2$, and KCl, Berndt et al. (1989) observed Na-metasomatism with a simultaneous decrease in the pH of the hydrothermal fluids. The Na-metasomatism became more important with increasing temperature and was significantly more important at 425°C than at 400°C (at 400 bar). We suggest that as temperature increases, there is a greater likelihood of Na-metasomatism. Although pressure is likely a determining factor in the exact reaction mechanism, the presence of molten rock provides sufficiently high temperatures to produce H^+ in either the gas or aqueous phase at the expense of Na^+.

7. CONCLUSIONS

In results presented here, Na-metasomatism and the release of magmatic gasses have been identified as the sources of acidic fluids generated by the reaction between molten rock and seawater. Approximately 30% of the acidity came from magmatic gasses with the balance from water–rock reactions, predominantly Na-metasomatism. When plotted versus water temperature, the chemical alterations observed in the experiments for pH, alkalinity, and F were similar to those observed in the surface ocean, suggesting that the experiments duplicated the natural process fairly well. This allows us to calculate a flux of acid from lava–seawater interactions at Kilauea. The experimental results show acid formation at a rate of 4 mEq per kilogram of lava, which based on lava extrusion rates for Kilauea discussed above (Kauahikaua et al., 1996; Harris et al., 1998) results in an acid formation rate of 200 to 700×10^6 Eq/year.

The occurrence of near-surface ocean volcanism has been a common phenomenon in the geologic past, suggesting the processes we have observed when molten lava and seawater interact were common phenomena in the ancient oceans. In discussing the environmental implications of the emplacement of large igneous provinces, one of the three effects that Coffin and Eldholm (1994) consider important is the "chemical and physical changes of the hydrosphere caused by the interaction of lava and seawater." A recent workshop on the effect of hydrothermal activity on primary production in the oceans concluded that only near-surface ocean hydrothermal activity was likely to contribute Fe and other nutrients to the photic zone (Kadko et al., 1999). At Kilauea and other surface ocean eruptions, the interaction between lava and seawater produces acid-rich aerosols also rich in Fe. These aerosols can be carried away from the site of the eruption and be deposited over the surface of the ocean. Fe is a limiting nutrient in the growth of oceanic phytoplankton (Martin et al., 1990) and its presence in trace amounts promotes primary productivity. To be used by the phytoplankton, however, the Fe must be in some labile phase and thus the deposition of volcanic glass may not promote primary productivity in the same manner as the deposition of Fe dissolved in an acidic fluid. In the case of an emergent volcanic island like Surtsey, the 1- to 2-km height of the eruption plume would allow for the deposition of dissolved Fe over great distances. However, the volcanism that takes place near the surface of the ocean is typically explosive in nature (Cas, 1992) creating rapidly cooled hyaloclastic materials, and thus the reaction between seawater and lava must take place in a small window of time. As a result, the hyloclastites produced in the near-surface ocean are not likely to be altered by longer term high-temperature hydrothermal reactions like those observed at MOR spreading centers but instead are likely to experience reactions like those reported here. The fast nonequilibrium reaction between lava and seawater in the surface ocean will, therefore, release less Fe than would be released from

Table 7. Average values of acid generated for different experiments.

Average value for all experiments containing NaCl*	(n = 4)	3.3 ± 1.4
SW Day-2	(n = 4)	2.9 ± 0.7
SW Day-1	(n = 6)	5.0 ± 1.1
Average value for all SW experiments	(n = 10)	4.0 ± 1.5
August DIW	(n = 5)	0.8 ± 0.4
October DIW	(n = 4)	1.3 ± 0.3
Average value for all DIW experiments	(n = 9)	1.0 ± 0.5

* From Table 2.

longer term near-equilibrium hydrothermal process like those observed at MORs.

Presently, 80% of the annual volcanism takes place beneath the surface of the ocean at MOR spreading centers and at intraplate submarine volcanos (Crisp, 1984) where the pressure is generally much higher than that in the surface ocean. These eruptions are often preceded by the intrusion of magma into existing hydrothermal reservoirs as has been proposed for the formation of mega-plumes above areas of recent magmatic activity (Baker et al., 1989; Lowell and Germanovich, 1995). These reservoirs may contain hydrothermally altered Mg-replete fluids similar to the fluids used in experimental studies where Na-metasomatism was observed (Berndt et al., 1989) or may contain interstitial waters closer in composition to seawater. In either case, the elevated temperatures and rapid reaction kinetics present during magma-seawater interaction may favor short-term Na-metasomatism. In addition, the high temperatures associated with the intrusion of magma into a hydrothermal system leads to phase separation of the fluids (e.g., Massoth et al., 1989; Von Damm et al., 1997) forming both brine and vapor phases. In addition to brine and vapor, it has been hypothesized that halite was deposited within the 9 to 10°N hydrothermal system during eruption (Berndt and Seyfried, 1997). This is supported by the observation of deposits of solid halite on pillow lavas (Butterfield et al., 1997) and on glass shards suspended in the water column (R. Feely, pers. comm.) at sites of recent submarine eruptions. The short-lived environments where halite was deposited may correspond to places where molten rock and seawater came in contact. The presence of vapor and solid halite show that an environment similar to that observed at the shoreline of Kilauea can be present in the deep ocean.

The observation of Na-metasomatism at 425°C and 400 bars (Berndt et al., 1989) suggests that Na-metasomatism may be driven mostly by high temperatures with pressure being a less important factor. In the deep ocean, the presence of molten rock creates reaction conditions with very high temperatures, most likely leading to the immediate formation of acid. Acidic solutions uniformly strip cations from basalt glass (e.g., Gout et al., 1997) generating a hydrothermal solution with a different chemical signature than that from near-equilibrium hydrothermal reactions. In the precipitation samples, for example, we observe Fe:Mn ratios of 54 ± 2 and Al:Mn ratios of 90 ± 2, which are much higher than the values observed in hydrothermal systems, where Fe:Mn ≈ 0.2 to 4:1 and Al:Mn ≈ 0.001 to 0.01:1. The observation of elevated Fe:Mn ratios in mega-plumes (e.g., Massoth et al., 1998) could have been brought about by a combination of eruption-influenced fluids and ordinary hydrothermal fluids. Similarly, during the Macdonald Seamount summit eruption, fluids were produced that had an Al:Mn ratio of ~5:1 and an Fe:Mn ratio of ~33:1 (Resing et al., 1992), suggesting that the waters in the Macdonald plume may also have been an admixture of eruption and hydrothermal fluids. Finally, Gamo et al. (1987) observed very high concentrations of Al^{3+} in hydrothermal plumes in the Manus Basin with Al:Mn ratios of ~15:1, which suggests that the hydrothermal fluids forming this plume may have been generated in part from an eruption.

The results presented here provide a framework to better understand and further study the interaction between molten rock and water. This interaction was certainly a very common one in the geologic past and continues to be common in the present. There is much research today aimed at understanding the evolution of MOR hydrothermal systems, and the evolution of MOR hydrothermal systems starts with the intrusion or eruption of magma into seawater. We can gain even more understanding by conducting hydrothermal experiments that address the kinetics of reaction at the high temperatures and pressures that must be present when lava at 1150°C comes in contact with seawater.

Acknowledgments—We thank G. Wheat, J. Plant, M. Bertram, T. Rust, G. Tribble, S. Reed, K. Kelly, and R. Kawamoto for field assistance. In particular we thank Jane Culp who participated in almost every field operation. In addition we acknowledge the assistance, guidance, and interpretation provided by the staff of the Hawaiian Volcano Observatory including D. Clague, T. Elias, T. Mattox, S. Mattox, J. Kauahikaua, and C. Thornber. We thank the Hawaii Volcanos National Park for granting access to the lava flows and the many different rangers at the park who kept an eye on our safety. We thank Dave Butterfield for providing additional data for the precipitation samples. Discussion with Y. H. Li, M. Mottl, S. Self, and C. Measures of the ideas presented in this manuscript were very helpful. In-depth reviews were provided by J. Bischoff, M. Berndt, and an anonymous reviewer. M. Berndt kindly discussed the manuscript and provided important ideas and thermodynamic calculations. Funding for this research was provided by the Office of Naval Research (N00014-96-10352 to J. Resing via Y. H. Li; N0014-90-J-1805 and N00014-94-1-0631 to F. J. Sansone) and the National Science Foundation (OCE-9314394 to F. J. Sansone). This is SOEST Contribution No. 4826 and PMEL Publication No. 2062.

REFERENCES

Armellini F. J. and Tester J. W. (1993) Solubility of sodium chloride and sulfate in sub- and supercritical water vapor from 450–550°C and 100–250 bar. *Fluid Phase Equil.* **84,** 123–142.

Baker E. T., Lavelle J. W., Feely R. A., Massoth G. J., and Walker S. L. (1989) Episodic venting of hydrothermal fluids from the Juan de Fuca Ridge. *J. Geophys. Res.* **94,** 9237–9250.

Berndt M. E. and Seyfried W. E. (1997) Calibration of Br/Cl fractionation during subcritical phase separation of seawater: Possible halite at 9–10°N East Pacific Rise. *Geochim. Cosmochim. Acta* **61,** 2849–2854.

Berndt M. E., Seyfried W. E., and Janecky D. R. (1989) Plagioclase and epidote buffering of cation ratios in mid-ocean ridge hydrothermal fluids: Experimental results in and near the supercritical region. *Geochim. Cosmochim. Acta* **53,** 2283–2300.

Beirsdorf H., Bach W., Duncan R., Erzinger J., and Weiss W. (1995) New evidence for the production of EM-type ocean island basalts during the early history of the Manihiki Plateau. *Mar. Geol.* **122,** 181–205.

Bischoff J. L. and Dickson F. W. (1975) Seawater–basalt interaction at 200°C and 500 bars: Implications for origin of sea-floor heavy-metal deposits and regulation of seawater chemistry. *Earth Planet. Sci. Lett.* **25,** 385–397.

Bischoff J. L., Rosenbauer R. J., and Fournier R. O. (1996) The

generation of HCl in the system $CaCl_2$–H_2O: Vapor–liquid relations from 380–500°C. *Geochim. Cosmochim. Acta* **60,** 7–16.

Butterfield D. A. and Massoth G. J. (1994) Geochemistry of north cleft segment vent fluids: Temporal changes in chlorinity and their possible relation to recent volcanism. *J. Geophys. Res.* **99,** 4951–4968.

Butterfield D. A., Massoth G. J., McDuff R. E., Lupton J. E., and Lilley M. D. (1990) Geochemistry of hydrothermal fluids from Axial Seamount hydrothermal emissions study vent field, Juan de Fuca Ridge: Subseafloor boiling and subsequent fluid-rock interaction. *J. Geophys. Res.* **95,** 12895–12921.

Butterfield D. A., Jonasson I. R., Massoth G. J., Feely R. A., Roe K. K., Embley R. E., Holden J. F., McDuff R. E., Lilley M. D., and Delaney J. R. (1997) Seafloor eruptions and the evolution of hydrothermal chemistry. *Phil. Trans. R. Soc. Lond. A.* **355,** 369–386.

Cas R. A. F. (1992) Submarine volcanism: Eruption styles, products, and relevance to understanding the host-rock successions to volcanic-hosted massive sulfide deposits. *Econ. Geol.* **87,** 511–541.

Cashman K. V., Mangan M. T., and Newman S. (1994) Surface degassing and modifications to vesicle size distributions in active basalt flows. *J. Volc. Geotherm. Res.* **61,** 45–68.

Cheminée J.-L., Stoffers P., McMurtry G., Richnow H., Puteanus D., and Sedwick P. (1991) Gas-rich submarine exhalations during the 1989 eruption of Macdonald Seamount. *Earth Planet. Sci. Lett.* **107,** 318–327.

Clews F. H. and Thompson H. V. (1922) The interaction of sodium chloride and silica. *J. Chem. Soc.* **V121,** 1443–1448.

Coffin M. F. and Eldholm O. (1994) Large igneous provinces: Crustal structure, dimensions, and external consequences. *Rev. Geophys.* **32,** 1–36.

Crisp J. A. (1984) Rates of magma emplacement and volcanic output. *J. Volc. Geotherm. Res.* **20,** 177–211.

Dove P. M. and Crerar D. A. (1990) Kinetics of quartz dissolution in electrolyte solutions using a hydrothermal mixed flow reactor. *Geochim. Cosmochim. Acta* **54,** 955–969.

Duennebier F. K., Becker N. C., Caplan-Auerbach J., Clague D. A., Cowen J., Cremer M., Garcia M., Goff F., Malahoff A., McMurtry G. M., Midson B. P., Moyer C. L., Norman M., Okubo P., Resing J. A., Rhodes J. M., Rubin K., Sansone F. J., Smith J. R., Spencer K., Wen X., and Wheat C. G. (1997) Researchers rapidly respond to submarine activity at Loihi Volcano, Hawaii. *EOS Trans. Am. Geophy. Un.* **78,** 22, 229, 232–233.

Edmond J. M. (1970) High precision determination of titration alkalinity and total carbon dioxide content of seawater by potentiometric titration. *Deep Sea Res.* **17,** 737–750.

Eldholm O. and Thomas E. (1993) Environmental impact of volcanic margin formation. *Earth Planet. Sci. Lett.* **117,** 319–329.

Fournier R. O. and Thompson J. M. (1993) Composition of steam in the system NaCl-KCl-H_2O-quartz at 600°C. *Geochim. Cosmochim. Acta* **57,** 4365–4375.

Froelich P. N., Kim K. H., Burnett W. C., Jahnke R., Soutar A., and Deakin M. (1983) Pore water fluoride in Peru continental margin sediments: Uptake from seawater. *Geochim. Cosmochim. Acta* **47,** 1605–1612.

Galobardes J. F., Van Hare D. R., and Rogers L. B. (1981) Solubility of chloride in dry steam. *J. Chem. Eng. Data* **26,** 363–366.

Gamo T., Ishibashi J-I, Sakai H., and Tilbrook B. (1987) Methane anomalies in seawater above the Loihi submarine summit area, Hawaii. *Geochim. Cosmochim. Acta* **51,** 2857–2864.

Geiskes J. and Peretsman G. (1986) *Water-chemistry procedures aboard the Joides Resolution—Some comments*. Ocean Drilling Program Technical Note #5.

Gerlach T. M. (1993) Oxygen buffering of Kilauea gases and the oxygen fugacity of Kilauea basalt. *Geochim. Cosmochim. Acta* **57,** 795–814.

Gerlach T. M. and Taylor B. E. (1990) Carbon isotope constraints on degassing of carbon dioxide from Kilauea Volcano. *Geochim. Cosmochim. Acta* **54,** 2051–2058.

Gerlach T. M., Krumhansl J. L., Fournier R. O., and Kjargaard J. (1989) Acid rain from the heating of seawater by molten lava: A new volcanic hazard. *EOS* **70,** 1421–1422 (abstr).

Gout R., Oelkers E. H., Schott J., and Zwick A. (1997) The surface chemistry of acid-leached albite: New insights on the dissolution mechanism of the alkali feldspars. *Geochim. Cosmochim. Acta* **61,** 3013–3018.

Govindaraju K. (1989). 1989 compilation of working values and sample description for 272 geostandards. *Geost. Newslett.* **13,** 1–113.

Greenland L. P. (1984) Gas composition of the January 1983 eruption of Kilauea Volcano, Hawaii. *Geochim. Cosmochim. Acta* **48,** 193–195.

Greenland L. P., Rose W. I., and Stokes J. B. (1985) An estimate of gas emissions and magmatic gas content from Kilauea Volcano. *Geochim. Cosmochim. Acta* **49,** 125–129.

Hanf N. W. and Sole M. J. (1970) High temperature hydrolysis of sodium chloride. *Trans. Faraday Soc.* **66,** 3065–3074.

Harris A. J. L., Flynn L. P., Rowland S. K., Keszthelyi L., Mouginis-Mark P. J., and Resing J. A. (1998) Calculation of lava effusion rates from Landsat-TM data. *Bull. Volc.* **60**(1), 52–71.

Heliker C. and Wright T. L. (1991) The Pu'u O'o-Kupaianaha eruption of Kilauea. *EOS Trans. AGU* **72,** 521, 526, 530.

Helz R. T., Banks N. G., Heliker C., Neal C. A., and Wolfe E. W. (1995) Comparative geothermometry of recent Hawaiian eruptions. *J. Geophys. Res.* **100,** 17637–17657.

Holbrook W. S. and Kelemen P. B. (1993) Large igneous province on the US Atlantic margin and implications for magmatism during continental breakup. *Nature* **364,** 433–436.

Kadko D., Baross J., and Baker E. (1999) *Workshop Report on the Effect of Seafloor Hydrothermalism on Surface Ocean Productivity*. RIDGE publications, Corvalis, OR.

Kauahikaua J., Mangan M., Heliker C., and Mattox T. (1996) A quantitative look at the demise of a basaltic vent: The death of Kupaianaha, Kilauea Volcano, Hawaii. *Bull. Volc.* **57,** 641–648.

Kelly K. M., Hon K., and Tribble G. W. (1989) Bathymetric and submarine studies of an active lava delta near Kupapau Point, Kilauea Volcano, Hawaii. *EOS* **70,** 1202 (abstr.).

Kokelar P. (1986) Magma–water interactions in subaqueous and emergent basaltic volcanism, *Bull. Volc.* **48,** 275–289.

Langmuir D. (1997) *Aqueous Environmental Geochemistry*. Prentice-Hall.

Lowell R. P. and Germanovich L. N. (1995) Dike injection and the formation of megaplumes at ocean ridges. *Science* **267,** 1804–1807.

Martin J. H., Gordon R. M., and Fitzwater S. E. (1990) Iron in Antarctic waters. *Nature* **345,** 156–158.

Massoth G. J., Butterfield D. A., Lupton J. E., McDuff R. E., Lilley M. D., and Jonasson I. R. (1989) Submarine venting of phase-separated hydrothermal fluids at Axial Volcano, Juan de Fuca Ridge. *Nature* **340,** 702–705.

Massoth G. J., Baker E. T., Feely R. A., Lupton J. E., Collier R. W., Gendron J. F., Roe K. K., Maenner S. M., and Resing J. A. (1998) Manganese and iron in hydrothermal plumes resulting from the 1996 Gorda Ridge Event. *Deep Sea Research II* **45,** 2683–2712.

Mattox T. N., Heliker C., Kauahikaua J., and Hon K. (1993) Development of the 1990 Kalapana flow field, Kilauea Volcano, Hawaii. *Bull. Volc.* **55,** 407–413.

Meunow D. W., Graham D. G., and Liu N. W. K. (1979) The abundance of volatiles in Hawaiian Tholeiitic submarine basalts. *Earth Planet. Sci. Lett.* **42,** 71–76.

Miller T. L., Zoller W. H., Crowe B. M., and Finnegan D. L. (1990) Variations in trace metal and halogen ratios in magmatic gases through an eruptive cycle of the Pu'u O'o vent, Kilauea, Hawaii: July–August 1985. *J. Geophys. Res.* **95,** 12607–12615.

Mottl M. J. and Holland H. D. (1978) Chemical exchange during hydrothermal alteration of basalt by seawater—I. Experimental results for major and minor components of seawater. *Geochim. Cosmochim. Acta* **42,** 1103–1115.

Peterson D. W. (1976) Processes of volcanic island growth, Kilauea Volcano, Hawaii, 1969–1973. Paper presented at the Symposium on Andean and Antarctic Volcanology Problems, Int. Assoc. of Volcanol. and Chem. of the Earth's Interior, Santiago, Chile.

Peterson D. W., Holcomb R. T., Tilling R. I., and Christiansen R. L. (1994) Development of lava tubes in the light of observations at Mauna Ulu, Kilauea Volcano, Hawaii. *Bull. Volc.* **56,** 343–360.

Resing J. A. (1997) The chemistry of lava–seawater interactions at the shoreline of Kilauea Volcano, Hawaii. PhD dissertation, Univ. Hawaii.

Resing J. A. and Measures C. I. (1994) Fluorometric determination of

Al in seawater by flow injection analysis with in-line preconcentration. *Anal. Chem.* **66,** 22, 4105–4111.

Resing J. A. and Sansone F. J. (1996) Al and pH anomalies in the Manus Basin reappraised: Comments on the paper by T. Gamo et al., Hydrothermal plumes in the eastern Manus Basin, Bismarck Sea: CH_4, Mn, Al, and pH anomalies. *Deep Sea Res.* **43,** 1867–1872.

Resing J. A., Sansone F. J., Wheat C. G., Measures C. I., McMurtry G. M., Sedwick P. N., and Massoth G. J. (1992) The extraction of aluminum from hot rock: The elemental signature of an eruptive vs. classical hydrothermal system. *EOS* **73,** 254 (abstr.).

Rimstidt J. D. and Barnes H. L. (1980) The kinetics of silica–water reactions. *Geochim. Cosmochim. Acta* **44,** 1683–1699.

Rowe J. J., Fournier R. O., and Morey G. W. (1967) The system water–sodium oxide–silicon dioxide at 200, 250, and 300°. *Inorg. Chem.* **6,** 6, 1183–1188.

Sansone F. J. and Resing J. A. (1995) Hydrography and geochemistry of sea surface hydrothermal plumes resulting from Hawaiian coastal volcanism. *J. Geophys. Res.* **100,** c7, 13555–13569.

Schlanger S. O., Jenkyns H. C., and Premoli-Silva I. (1981) Volcanism and vertical tectonics in the Pacific Basin related to global Cetaceous transgressions. *Earth Planet. Sci. Lett.* **52,** 435–449.

Sedwick P. N., McMurtry G. M., and Tribble G. W. (1991) Chemical alteration of seawater by lava from Kilauea Volcano, Hawaii. *Mar. Geol.* **96,** 151–158.

Sedwick P. N., McMurtry G. M., and Macdougall J. D. (1992) Chemistry of hydrothermal solutions from Pele's Vents, Loihi Seamount, Hawaii. *Geochim. Cosmochim. Acta* **56,** 3643–3667.

Seyfried W. E. and Janecky D. R. (1985) Heavy metal and sulfur transport during subcritical and supercritical hydrothermal alteration of basalt: Influence of fluid pressure and basalt composition and crystallinity. *Geochim. Cosmochim. Acta* **49,** 2545–2560.

Seyfried W. E. and Mottl M. J. (1995) Geologic setting and chemistry of deep-sea hydrothermal vents. In *Deep-Sea Hydrothermal Vents* (ed. D. Karl). CRC Press.

Shanks W. C. III and Seyfried W. E. Jr. (1987) Stable isotopes of vent fluids and chimney minerals, Southern Juan de Fuca Ridge: Sodium metasomatism and seawater sulfate reduction. *J. Geophys. Res.* **92,** 11387–11399.

Symonds R. B., Rose W. I., Bluth G. J. S., and Gerlach T. M. (1994) Volcanic–gas studies: Methods, results and applications. In *Volatiles in Magmas* (ed. M. R. Carroll and J. R. Holloway), pp. 1–66. Min. Soc. Am.

Tarduno J. A., Sliter W. V., Kroenke L., Leckie M., Mayer H., Mahoney J. J., Musgrave R., Storey M., and Winterere E. L. (1991) Rapid formation of the Ontong java Plateau by Aptian mantle plume volcanism. *Science* **254,** 399–403.

Tester J. W., Worley W. G., Robinson B. A., Grigsby C. O., and Feerer J. L. (1994) Correlating quartz dissolution kinetics in pure water from 25–625°C. *Geochim. Cosmochim. Acta* **58,** 2407–2420.

Trefry J. H., Butterfield D. A., Metz S., Massoth G. J., Trocine R. P., and Feely R. A. (1994) Trace metals in hydrothermal solutions from cleft segment on the southern Juan de Fuca Ridge. *J. Geophys. Res.* **99,** 4925–4935.

Tribble G. W. (1991) Underwater observations of active lava flows from Kilauea Volcano, Hawaii. *Geology* **19,** 633–636.

Von Damm K. L. (1990) Seafloor hydrothermal activity: Black smoker chemistry and chimneys. *Ann. Rev. Earth Planet. Sci.* **18,** 173–204.

Von Damm K. L., Buttermore L. G., Oosting S. E., Bray A. M., Fornari D. J., Lilley M. D., and Shanks W. C. III. (1997) Direct observation of the evolution of a seafloor "black smoker" from vapor to brine. *Earth Planet. Sci. Lett.* **149,** 101–111.

Wallace P. and Carmichael I. S. E. (1992) Sulfur in basaltic magmas. *Geochim. Cosmochim. Acta* **56,** 1863–1874.

Warner T. B. (1971) Normal fluoride content of seawater. *Deep Sea Res.* **18,** 1255–1263.

Weast R. C. (1970) *CRC Handbook of Chemistry and Physics*. The Chemical Rubber Company.

Weiss R. F. and Craig H. (1973) Precise shipboard determination of dissolved nitrogen, oxygen, and argon in water and seawater. *Deep Sea Res.* **20,** 291–303.

White R. S. (1989) Asthenenosphere control on magmatism in the ocean basins. In *Magmatism in the Ocean Basins* (ed. A. D. Saunders and M. J. Norry), pp. 17–27. Geol. Soc. Spec. Pub. No. 42.

White R. and McKenzie D. (1989) Magmatism at rift zones: The generation of volcanic continental margins and flood basalts. *J. Geophys. Res.* **94,** 7685–7729.

Whitefield M., Leyendekkers V., and Kerr J. D. (1969) Liquid ion exchange electrodes as endpoint indicators in complexiметric titrations. *Anal. Chim. Acta* **45,** 399–410.

Wolfe E. W., Garcia M. O., Jackson D. B., Koyanagi R. Y., Neal C. A., and Okamura A. T. (1987) The Puu Oo eruption of Kilauea Volcano, episodes 1–20, January 3, 1983, to June 8, 1984. In *Volcanism in Hawaii* (ed. R. W. Decker et al.) pp. 471–508. U.S. Geol. Surv. Prof. Paper 1350.